Electrochemically produced battery-type $Ni(OH)_2/Ni_3Si$ electrodes

Kai Cui, Zhilong Zhao ✉*, Wenbin Liu*

School of Mechanical Engineering, Northwestern Polytechnical University, Xi'an 710072, People's Republic of China
✉ *E-mail: zhaolong@nwpu.edu.cn*

Published in Micro & Nano Letters; Received on 3rd June 2020; Revised on 9th July 2020; Accepted on 6th August 2020

The fabrication, by an electrochemical process, of a new battery-type electrode material, is presented. Such materials are fabricated by direct current electrodeposition of $Ni(OH)_2$ on lamellar Ni_3Si. Microstructure and morphology of $Ni(OH)_2/Ni_3Si$ electrodes were characterised. Cyclic voltammetry and galvanostatic charge–discharge results revealed that they are battery-type electrodes. Increasing deposition time or decreasing discharge current can significantly increase the areal capacity. The areal capacity of $Ni(OH)_2/Ni_3Si$-20 with a discharge current of 20 mA is only 2.8% of that with 1 mA. However, the increasing deposition time will reduce the cyclic stability of the electrodes. The initial areal capacity of $Ni(OH)_2/Ni_3Si$-20 is twice that of $Ni(OH)_2/Ni_3Si$-10 with a discharge current of 10 mA, but after 1000 cycles, it can only maintain 59.3% of the initial value. This Letter is expected to provide a powerful reference and guidance for the preparation of electrodes with large areal capacity and cycle stability.

1. Introduction: $Ni(OH)_2$, as a positive active material of nickel-based batteries, has many advantages such as large specific area and high electrochemical activity, which is particularly important for the capacity and service life of batteries [1, 2]. Therefore, preparation of $Ni(OH)_2$ cathode materials with high purity and activity has become a hot research topic in recent years. At present, the synthesis methods of $Ni(OH)_2$ include chemical precipitation method, precipitation conversion method, oxidation method and so on [3–5]. Most of the prepared $Ni(OH)_2$ powders are of poor uniformity, poor crystal form, which directly affect the performance of $Ni(OH)_2$ as an active material. Furthermore, $Ni(OH)_2$ material is a semiconductor whose poor conductivity also affects the reliability and discharge properties of its electrodes application [6]. Selecting materials with good conductivity as substrate to carry $Ni(OH)_2$ is an excellent solution for these problems, which can greatly improve the conductivity while achieving good dispersion. Lamellar Ni_3Si obtained by the combination of directional solidification and selective corrosion in our laboratory presented a good conductivity, high mechanical strength and corrosion resistance to acid and alkali [7–9].

In this work, a novel electrochemically produced battery-type electrode material was presented. Lamellar Ni_3Si with controllable microgrooves was used as the substrate material for electrode preparation, and $Ni(OH)_2$ was loaded on the substrate by electrodeposition with different deposition time. Results of cyclic voltammetry (CV) and galvanostatic charge–discharge (GCD) measurements indicated that the combination of Ni_3Si substrate and $Ni(OH)_2$ can obtain a large areal capacity while maintaining high cyclic stability.

2. Experimental: The lamellar Ni_3Si substrate was prepared through the directional solidification of Ni-Ni_3Si eutectic alloy and the subsequent selective corrosion of Ni phase as reported in our previous works [7–9]. In this Letter, the lamellar Ni_3Si prepared with a directional growth rate of 10 μm/s and a corrosion time of 1 h was selected as the substrate for deposition. Before the synthesis of $Ni(OH)_2/Ni_3Si$ electrodes, the selected Ni_3Si substrates were manually sampled, ultrasonically washed with distilled water followed by rinsing with ethanol, and finally dried at room temperature. The typical electrodeposit procedure of $Ni(OH)_2$ was conducted in a standard three-compartment cell on a CS350 (CorrTest, China) electrochemical workstation. A Pt foil with a surface area of 2 cm^2 and a saturated calomel electrode (SCE) were used as the counter and reference electrodes, respectively. The electrolyte for deposition of $Ni(OH)_2$ active material was prepared by dissolving 8.724 g (0.03 mol) $Ni(NO_3)_2{\cdot}6H_2O$ in 300 ml deionised water, and vigorously stirred to form a homogeneous solution. The electrochemical deposition experiments were conducted via a potentiostatic mode with a cathodic potential of $-0.7\ V_{SCE}$ [10]. Thereafter, $Ni(OH)_2$ was grown in situ on the Ni_3Si substrate. As a result, $Ni(OH)_2/Ni_3Si$ electrodes were successfully obtained and denoted as $Ni(OH)_2/Ni_3Si$-10, $Ni(OH)_2/Ni_3Si$-15, $Ni(OH)_2/Ni_3Si$-20, respectively, according to the deposition time (min). Finally, the prepared $Ni(OH)_2/Ni_3Si$ electrodes were rinsed several times with deionised water for subsequent measurements.

The phase constituents of the prepared Ni_3Si and $Ni(OH)_2/Ni_3Si$ electrodes were characterised through X-ray diffraction on a D8 Discover A25 diffractometer using a Co-Ka radiation source. The microstructures and morphologies of the prepared electrodes were characterised using a desktop scanning electron microscope (SEM, TM4000PLUS, HITACHI) system in backscattering mode.

CV and GCD measurements were carried out in 1 M NaOH aqueous solution using the above electrochemical workstation at room temperature. The CV curves were examined in the voltage window from 0 to $0.5\ V_{SCE}$ with different scan rates of 2, 5, 10 and 20 mV/s, and the GCD curves were collected with GCD currents of 1, 5, 10, 15 and 20 mA. The areal capacity, based on the geometric area of the electrodes, was calculated by the following equation according to the GCD curves [9]:

$$Q_s = \frac{I \times \Delta t}{3.6 \times S_0} \tag{1}$$

where Q_s, I, Δt and S_0 are the areal capacity ($mAhcm^{-2}$), discharge current (A), discharge time (s) and the geometric area (cm^2) of the electrodes, respectively.

3. Results and discussion: The morphologies of the as-prepared Ni_3Si and $Ni(OH)_2/Ni_3Si$ electrodes were examined by SEM, as shown in Figs. 1*a–h*. It can be seen that the surface morphology of Ni_3Si substrate has changed greatly after the deposition of $Ni(OH)_2$. The plane view and the enlarged partial view (Fig. 1*a*) show that the Ni_3Si substrate possesses a sandwiched structure with a lamellar space of 5.75 μm and a corrosion depth of 12.9 μm, which provides paths for transportation of both electrons and ions in the electrolyte, resulting in the improved

© The Institution of Engineering and Technology 2020

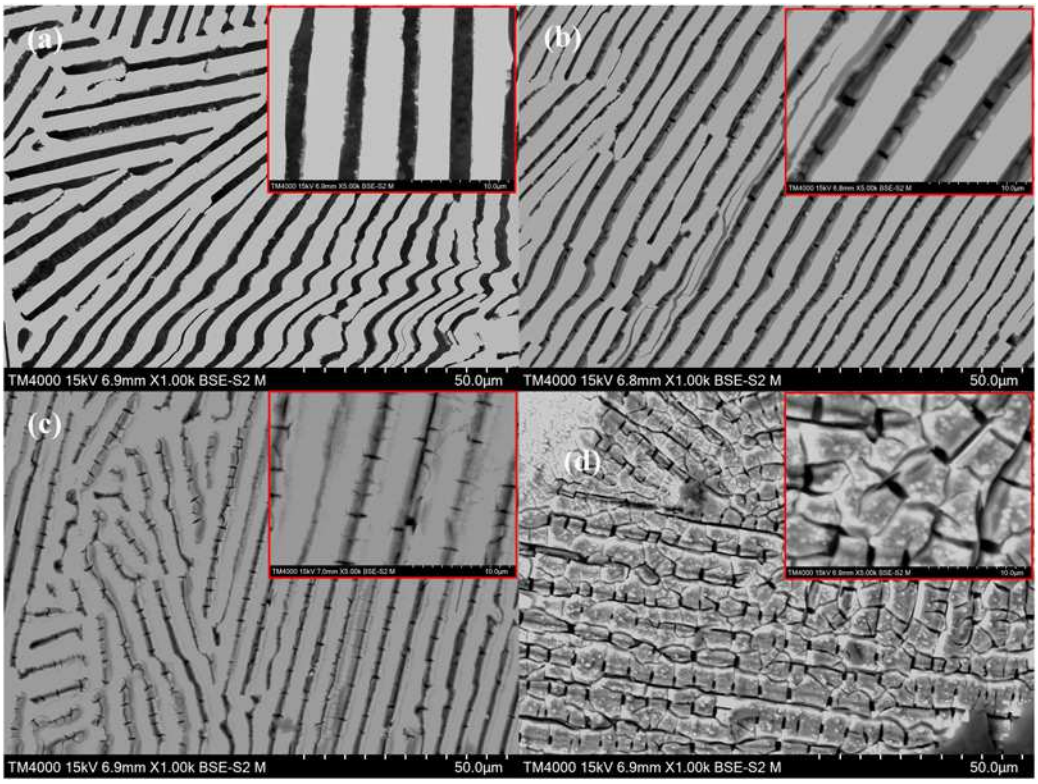


Fig. 1 *SEM images of*
a Ni_3Si electrode
b $Ni(OH)_2/Ni_3Si$-10 electrode
c $Ni(OH)_2/Ni_3Si$-15 electrode
d $Ni(OH)_2/Ni_3Si$-20 electrode

electrochemical performance. After electrodeposition for 10 min, $Ni(OH)_2$ was accumulated at the bottom of Ni_3Si substrate, as seen in Fig. 1*b*. Further increasing the deposition time, Ni $(OH)_2$ gradually filled the microgrooves and began to deposit on the surface of Ni_3Si substrate (Fig. 1*c*). After the deposition time reaches 20 min, the $Ni(OH)_2$ deposited can completely cover the surface of Ni_3Si substrate, with sparse gaps (Fig. 1*d*). This electrode structure can ensure fast ion/electron transfer, short ion transport distances and sufficient contact at active interfaces, which might improve the electrochemical performance.

The typical XRD patterns of the prepared Ni_3Si and $Ni(OH)_2/Ni_3Si$ electrodes are shown in Fig. 2. The diffraction peak positions of the four curves are almost the same, with only a difference in intensity. The original Ni_3Si substrate presents diffraction peaks besides Ni_3Si. This is caused by the corrosion mechanism of Ni_3Si template: the directional solidified Ni-Ni_3Si is composed of Ni phase and Ni_3Si phases. The selective corrosion of Ni phase will leave $Ni(OH)_2$, NiO_2 and other heterophases (not marked) in the microgroove. Since the corrosion time is only 1 h, the Ni phase has not been completely removed, and strong Ni peaks can still be detected. After deposition, the microgrooves formed after the corrosion of Ni phase were gradually covered by $Ni(OH)_2$, and the diffraction peaks representing the $Ni(OH)_2$ phases were relatively enhanced, while the intensity of the Ni phase was weakened to almost disappear, suggesting the successful synthesis of $Ni(OH)_2$ upon the Ni_3Si substrate.

The electrochemical performances of the prepared electrodes were examined systematically by CV and GCD measurements with a three-electrode cell in 1 M NaOH aqueous solution at room temperature (Fig. 3). The CV curves of the prepared Ni_3Si and $Ni(OH)_2/Ni_3Si$ electrodes with a scan rate of 10 mV/s within the potential window from 0 to 0.5 V are shown in Fig. 3*a*.

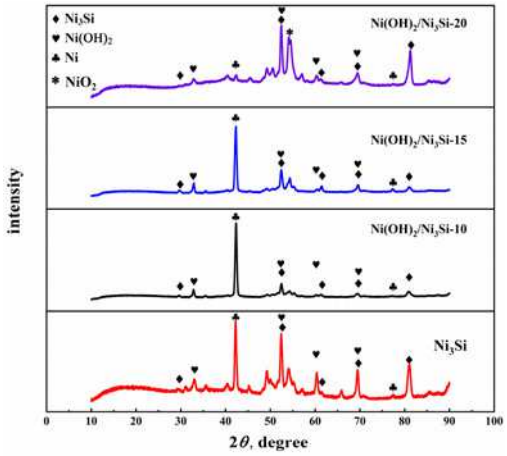


Fig. 2 *XRD pattern of the prepared Ni_3Si and $Ni(OH)_2/Ni_3Si$ electrodes*

The redox peaks illustrate that pseudo-capacitive behaviour occurred at the electrode/electrolyte interface. It is notable that with the increasing deposition time, the corresponding anode peak is shifted to a more positive value, which is related to the poor conductivity of $Ni(OH)_2$. GCD curves measured at a GCD current of 5 mA demonstrate that the prepared electrodes are battery-type materials, as shown in Fig. 3*b*. Every GCD curve has an obvious charge and discharge plateau and the voltage position is in agreement with the CV curves. The areal capacities of the electrodes were calculated from (1). The $Ni(OH)_2/Ni_3Si$-20 electrode presented the highest value of 3.65 $mAhcm^{-2}$, which is more than 200 times that of the Ni_3Si electrode. Fig. 3*c* discloses

© The Institution of Engineering and Technology 2020

doi: 10.1049/mnl.2020.0316

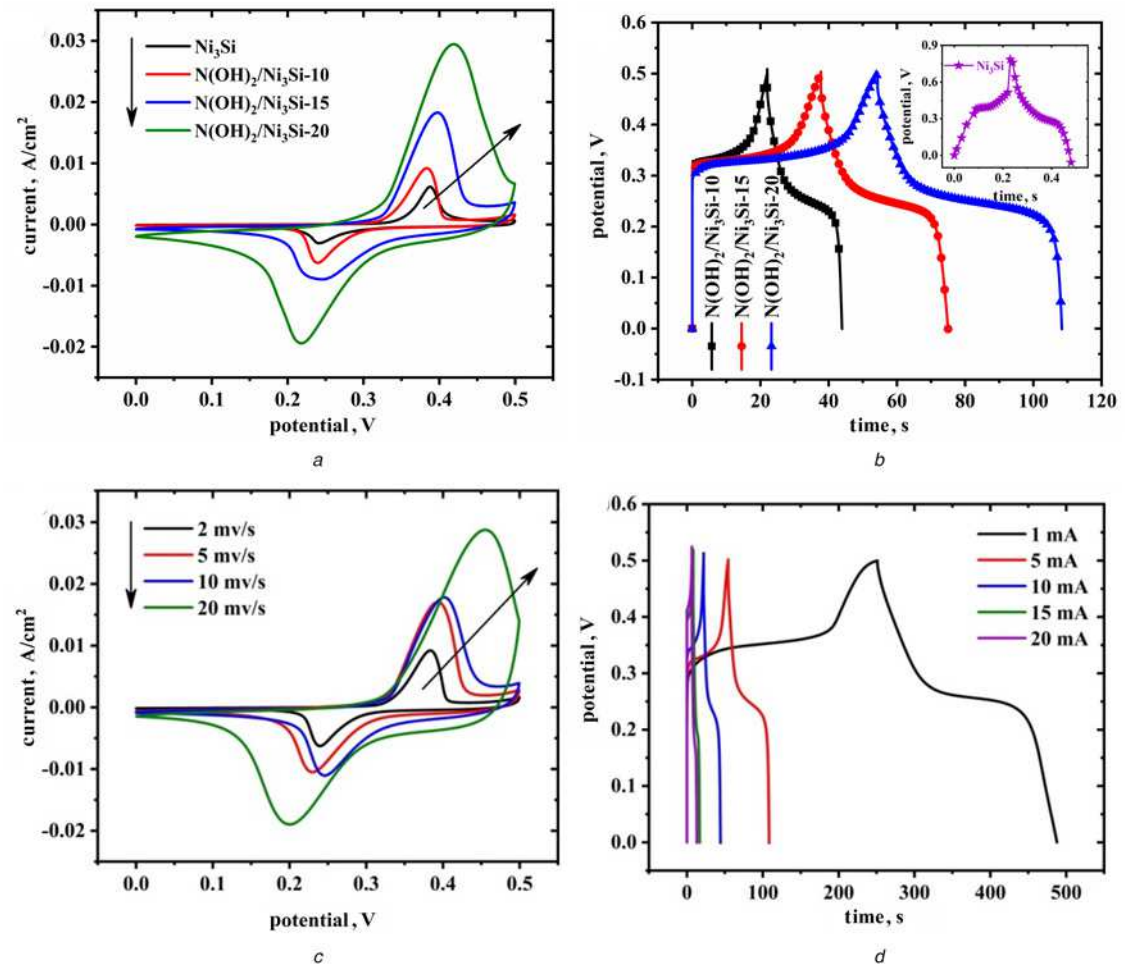


Fig. 3
a CV curves with a scan rate of 10 mV/s
b GCD curves with a current of 5 mA
c CV curves of $Ni(OH)_2/Ni_3Si$-20 electrode with different scan rates
d GCD curves of $Ni(OH)_2/Ni_3Si$-20 electrode with different currents

the CV responses of $Ni(OH)_2/Ni_3Si$-20 electrode with different scan rates ranging from 2 to 20 mV/s. The results indicate that the current response increases with the scan rate. Due to electrochemical polarisation, the cathode/anode peak of the curves was shifted to a more negative/positive directions with the increasing scan rate. The GCD curves for the $Ni(OH)_2/Ni_3Si$-20 electrode were recorded at different GCD currents from 1 to 20 mA (Fig. 3*d*). As the GCD current increases, the GCD curve shrinks significantly, due to less electroactive materials being available because of limited ion diffusion when the discharge current density increases. The areal capacities of the $Ni(OH)_2/Ni_3Si$-20 electrode are found to be 15.98, 3.65, 1.5, 0.57 and 0.45 $mAhcm^{-2}$ at discharge currents of 1, 5, 10, 15 and 20 mA, respectively. The rate performance is not ideal, proving that it is more suitable for applications under small current conditions.

Cycle performance is another key factor affecting the practical application of electrode materials [11]. The cycling stability (Fig. 4) of the prepared Ni_3Si and $Ni(OH)_2/Ni_3Si$ electrodes was evaluated by the continuous GCD measurement up to 1000 cycles with a GCD current of 10 mA. As shown in Fig. 4, the areal capacity of Ni_3Si electrode observed a significant increase due to the initial activation [12]. The initial area capacity is only 0.02 $mAhcm^{-2}$, which reaches 0.11 $mAhcm^{-2}$ after 600 cycles and then tends to be stable. The incorporation between Ni_3Si substrate and electroactive $Ni(OH)_2$ reversed the increasing trend. The areal capacity of $Ni(OH)_2/Ni_3Si$ electrodes decreases gradually

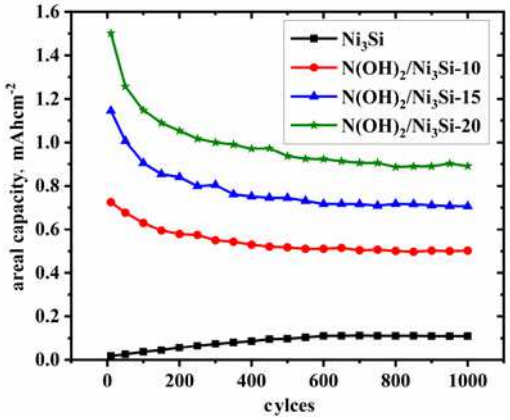


Fig. 4 *Cyclic stability of the prepared Ni_3Si and $Ni(OH)_2/Ni_3Si$ electrodes with a discharge current of 10 mA*

without activation process. The $Ni(OH)_2/Ni_3Si$-10 electrode has the highest cyclic stability, with a capacity loss of only 30.7% after 1000 cycles, but its initial areal capacity is only 0.72 $mAhcm^{-2}$. With the increase of deposition time, the areal capacity increases continuously, but the cycling stability decreases gradually. The $Ni(OH)_2/Ni_3Si$-20 electrode delivers a relatively high areal capacity

© The Institution of Engineering and Technology 2020

of 1.5 mAhcm^{-2} with 59.3% retention of its initial capacity after 1000 cycles. The cycle stability of $Ni(OH)_2/Ni_3Si$ electrodes has obvious advantages over the existing literature that using $Ni(OH)_2$ as active material. For example, a previous study observed that after 500 cycles the specific capacitance of $Ni(OH)_2$/graphene/nickel foam maintains 63% of the initial value [10]. This clearly demonstrate that the Ni_3Si substrate is beneficial to the cycling stability of $Ni(OH)_2$ electrodes.

4. Conclusion: A novel battery-type electrode material-$Ni(OH)_2/Ni_3Si$ was successfully manufactured by the electrodeposition approach. These electrodes contained a lamellar Ni_3Si structure which can provide a high mechanical strength substrate while improving the conductivity of $Ni(OH)_2$. The CV and GCD results demonstrate that the prepared Ni_3Si and $Ni(OH)_2/Ni_3Si$ are battery-type materials. The areal capacity of Ni_3Si observed a significant increase with the increasing GCD cycles, while those of the $Ni(OH)_2/Ni_3Si$ electrodes decrease gradually. With the increasing deposition time, the areal capacity of $Ni(OH)_2/Ni_3Si$ electrodes increases continuously, but the cyclic stability decreases. After 1000 cycles, the capacity loss of $Ni(OH)_2/Ni_3Si$-10 with a GCD current of 10 mA was 30.7%, but its initial areal capacity was only 48% that of $Ni(OH)_2/Ni_3Si$-20. The increase in discharge current limited the ion diffusion and decreased the areal capacity obviously. When the discharge current increases from 1 to 20 mA, the areal capacity of $Ni(OH)_2/Ni_3Si$-20 was decreased from 15.98 to 0.45 mAhcm^{-2}. The use of lamellar Ni_3Si as substrates for the electrochemical synthesis of electrode materials opens great promises for new nickel-based electrodes. Hopefully this Letter can provide a powerful reference and guidance for researchers who dedicate in the preparation of electrodes materials.

5. Acknowledgments: This work was supported by the National Natural Science Foundation of China (51374173), Natural Science Basic Research Plan in Shaanxi Province of China (2018JM5082) and Innovation Foundation for Doctor Dissertation of Northwestern Polytechnical University (CX201947).

6 References

[1] Watanabe K., Kikuoka T., Kumagai N.: 'Physical and electrochemical characteristics of nickel hydroxide as a positive material for rechargeable alkaline batteries', *J. Appl. Electrochem.*, 1995, **25**, (3), pp. 219–226

[2] Watanabe K., Koseki M., Kumagai N.: 'Effect of cobalt addition to nickel hydroxide as a positive material for rechargeable alkaline batteries', *J. Power Sources*, 1996, **58**, (1), pp. 23–28

[3] Wang T., Pan J.Q., Kiwanuka G.A., *ET AL.*: 'A green dual complexation precipitation synthesis of hierarchical α-$Ni(OH)_2$ microspheres and their electrochemical performance', *Int. J. Hydrog. Energy*, 2017, **42**, (30), pp. 19139–19147

[4] Reddy B.J., Vickraman P., Justin A.S.: 'Moringa oleifera leaf extract mediated reduced graphene oxide/α-$Ni(OH)_2$ nanocomposite for asymmetric supercapacitors', *Braz. J. Phys.*, 2019, **49**, (3), pp. 348–359

[5] Liu H., Xu J., Liu G.X., *ET AL.*: 'Building an interpenetrating network of $Ni(OH)_2$/reduced graphene oxide composite by a sol-gel method', *J. Mater. Sci.*, 2018, **53**, (21), pp. 15118–15129

[6] Zhang W.G., Jiao D.H., Yao Y., *ET AL.*: 'Electrochemical performance of $Ni(OH)_2$ positive materials', *Rare Metal Mater. Eng.*, 2014, **43**, (9), pp. 2055–2059

[7] Cui K., Zhao Z.L., Liu W.B.: 'Electrochemically prepared Ni_3Si with controllable areal capacity', *J. Electroanal. Chem.*, 2020, **865**, p. 114146

[8] Wei L.F., Zhao Z.L., Hu Z.R., *ET AL.*: 'Effect of growth rate on the microstructural transition and microhardness of directionally solidified Ni–11.8 wt% Si hypereutectic alloy', *J. Alloy. Compd.*, 2018, **742**, pp. 135–141

[9] Cui K., Zhao Z.L., Liu W.B.: 'Preparation, properties, and applications of lamellar Ni_3Si', *Metall. Mater. Trans A*, 2020, **51**, pp. 3365–3370

[10] Wang L.Q., Li X.C., Guo T.M., *ET AL.*: 'Three-dimensional $Ni(OH)_2$ nanoflakes/graphene/nickel foam electrode with high rate capability forsupercapacitor applications', *Int. J. Hydrogen Energy*, 2014, **39**, pp. 7876–7884

[11] Zheng D.H., Li M., Li Y.Y., *ET AL.*: 'A $Ni(OH)_2$ nanopetals network for high-performance supercapacitors synthesized by immersing Ni nanofoam in water', *Beilstein J. Nanotechnol.*, 2019, **10**, pp. 281–293

[12] Hu G., Tang C., Li C., *ET AL.*: 'The sol-gel-derived nickel-cobalt oxides with high supercapacitor performances', *J. Electrochem. Soc.*, 2011, **158**, (6), pp. A695–A699

© The Institution of Engineering and Technology 2020

doi: 10.1049/mnl.2020.0316